Sensor and Simulation Notes

Note 473

A Prototype High-Voltage UWB Transmitter

March 2003

Leland H. Bowen, Lanney M. Atchley, Everett G. Farr, and Donald E. Ellibee
Farr Research, Inc.

William J. Carey and Jon R. Mayes
Applied Physical Electronics, LC

Larry L. Altgilbers
U. S. Army / Space and Missile Defense Command

Abstract

We describe here the early development of a high-voltage Ultra-Wideband (UWB) transmitter that combines a collapsible Impulse Radiating Antenna and a fast-risetime triggered source. The antenna (TX-1) is a version of the CIRA-2 with a center support tube that should be large enough to eventually house a bipolar Marx generator. Applied Physical Electronics (APE) designed and built a prototype 400 kV bipolar Marx generator, which can be redesigned to fit into the TX-1 antenna. The bipolar Marx was developed because there is no room for a balun. The waveforms for both sides of the generator were measured, along with the jitter between the two sides. Low-voltage measurements on the antenna are also reported. We also experiment with a variety of unbalanced feed configurations, using a single 50-ohm cable to feed an 18-inch diameter IRA-2. Comparisons to the standard IRA-2 show only a modest degradation of the response below 12 GHz, in spite of the large impedance discontinuity at the feed point.

This work was funded in part by the Army Space and Missile Defense Command, Huntsville, AL, under contract DASG 60-02-0087.

1. Introduction.

We describe here the early development of a high-voltage Ultra-Wideband (UWB) transmitter that combines a portable high-gain antenna and a fast-risetime triggered source. The device, which is currently in the early stages of development, integrates a compact triggered wave-erection Marx generator into the center support of a Collapsible Impulse Radiating Antenna (CIRA). The antenna developed for this project is a modified version of the CIRA-2 manufactured by Farr Research. The center support tube of the CIRA-2 was greatly enlarged to provide space for the Marx generator. The current version of the antenna (TX-1) must be opened manually; however, a spring mechanism can be added to open the antenna automatically as it emerges from a housing. The Marx generator is a bipolar device with two outputs specifically designed for use on an Impulse Radiating Antenna (IRA).

We consider now the rationale for the configuration studied here. We want an integrated UWB source and antenna that can be stored in as small a space as possible, and that can be deployed automatically. So a collapsible antenna similar to our CIRA-2 seems appropriate. However, feeding such an antenna is a particular challenge. Normally an IRA includes a splitter balun that splits the signal from a 50-ohm source into two parallel 100-ohm cables, which are then connected in series at the feed point to drive the 200-ohm antenna. But such an arrangement is not practical in devices operating at high voltage within limited space, so we explore two options for avoiding the balun, a bipolar Marx generator and an unbalanced feed.

The first option for avoiding the balun was a bipolar Marx generator. This is just two identical Marx banks charged with equal and opposite polarities, timed to fire simultaneously, resulting in two equal and opposite outputs. With this configuration, each output can be used to drive half the antenna in a balanced configuration, since there is little jitter between the two outputs. This idea was conceived with the idea that most of the jitter between two Marx banks is determined by the time difference of the firing of the first gap. In the design used here, the first gap is shared by both Marx banks, so the jitter between the two sides should be minimal. We investigated this by building a prototype Bipolar Marx Generator that could demonstrate the principle. The prototype built here was too large to fit into our antenna, but it could be modified to fit in later versions. Our measurements showed a jitter of around 100 ps, which was a relatively small fraction of the risetime, so the device performed about as expected.

The second option for avoiding the balun was simply to use a single 50-ohm cable to drive the balanced 200-ohm antenna. To an antenna engineer, this is a rather unconventional approach, because we may drive the common mode in addition to the differential mode of the transmission line formed by the feed arms. Nevertheless, we thought that the simplest solution might work adequately in practice. To test the theory, we built a scale model 46 cm (18 in) in diameter. This was a version of the standard IRA-2 without the splitter balun feed, driven with a single 50-ohm cable connected across the feed point. The results show that even with the mismatch at the feed point, the performance of the antenna was only modestly degraded at frequencies below about 12 GHz. This more than covers the range of interest for the UWB transmitter, even after accounting for frequency scaling. While this type of feed cannot be used for applications such as radar, where reflections must be kept to a minimum, it can be used for other applications that are less sensitive to reflections.

In this report, we first describe the modified CIRA, the TX-1, and we show the results of the low-voltage antenna measurements. Next, we describe the bipolar Marx generator, and we provide results for that. Finally, we describe antenna experiments with two unbalanced feed configurations, using a single 50-ohm cable to feed an 18-inch diameter IRA-2.

2. TX-1 Antenna.

We provide here the design and measurements for the TX-1 collapsible antenna. The design was based on the CIRA-2 antenna manufactured by Farr Research, and it was intended to be integrated with the Marx generator described later. In this section, we describe the antenna and we provide results of low voltage measurements made on the Farr Research time domain antenna range.

2.1 TX-1 Antenna Description.

We begin by describing the details of the TX-1 antenna, pictures of which are shown in Figures 2.1 and 2.2. Both the CIRA-2 and the TX-1 are based on a 1.22 m (48 in) diameter parabolic reflector with a focal length of 0.488 m (F/D = 0.4). The reflector is sewn from 12 panels of a tough conductive mesh fabric, with an air permeability of approximately 3800 $ft^3/min./ft^2$. The reflector is supported on a frame of fiberglass rods attached to an aluminum center housing by aluminum pivots or hinges. The feed arms are fabricated from a combination of conductive and resistive fabrics. Both antennas have feed arms located at ±30° from the vertical, which is close to the optimal position[1, 2]. The CIRA-2 has a small-diameter aluminum tube as the center support for the feed point. However, the TX-1 has a center support fabricated from an aluminum tube with inner diameter of 102 mm (4 in) and outer diameter of 114 mm (4.5 in), which provides space for the bipolar Marx generator. An aluminum cone at the end of the Marx generator housing transitions to the feed point.

For this version of the TX-1 antenna, the standard feed arm configuration is used. In this configuration, part of the feed arms extend in front of a line between the focus and the reflector rim. This might make the fabric feed arms floppy, except that they are supported by an extra rod extending from the nearest rib. We considered using the "non-floppy design," in which the forward edge of the feed arms lay on a line from the focus to the rim of the reflector. This would eliminate the need for feed arm supports, but it would also move the inside edge of the feed arms 10 degrees closer to the center tube. The resulting close spacing could be a problem at high voltages.

When closed, the TX-1 (Figure 4.2) is 813 mm (32 in) long and 165 mm (6.5 in) in diameter. There is a wide point in the collapsed antenna that is caused by the pivots on the push rods that open the antenna. This wide point can be reduced by modifying the pivots, thereby reducing the diameter to about 152 mm. Also, the diameter of the center tube can probably be reduced when the size of the final version of the Marx is known. The final version of the bipolar Marx generator will probably be a folded design with two generators of opposite polarity side-by-side in the center tube. As we will see later, the bipolar output may not be required, because of the results of our unbalanced feeds described in Section 4. However, the total output voltage must be maintained, so more stages would have to be added to a single Marx. Thus, if we use a single-ended Marx the length would be increased and the diameter would be reduced.

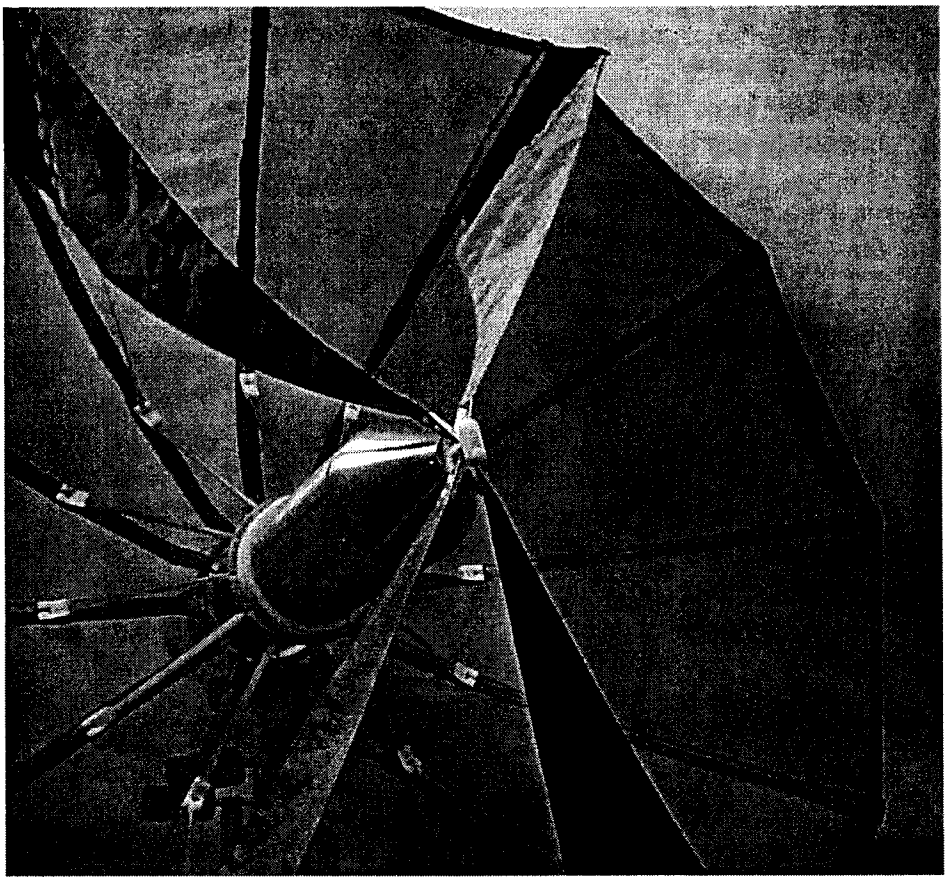

Figure 2.1. TX-1 antenna with large center tube.

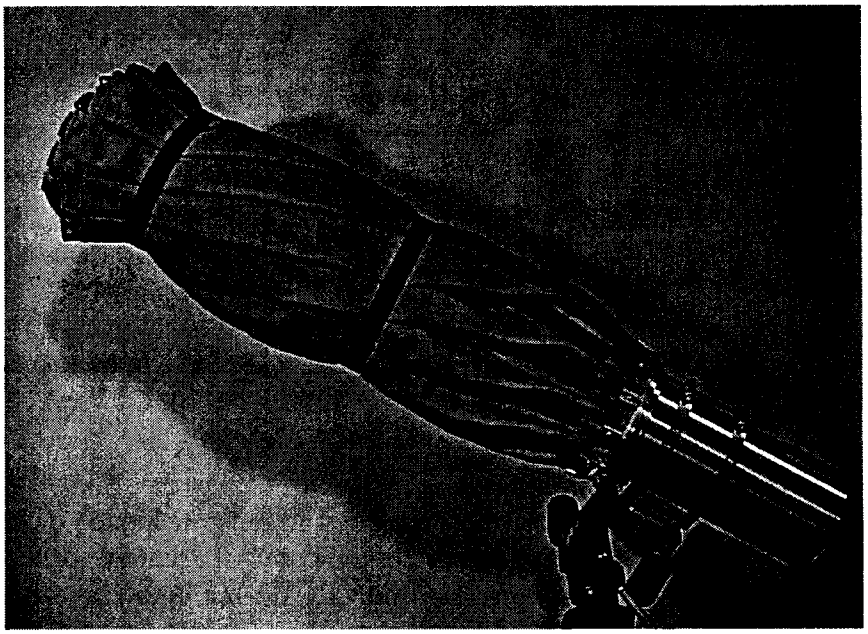

Figure 2.2. TX-1 antenna in closed configuration.

For the low-voltage measurements, the antenna was driven through a splitter that divided the signal from the 50-ohm source into two parallel 100-ohm cables. One of the cables normally runs down one of the feed arms and the other runs through the center support tube. However, in this case, both cables were run through the large center tube and were connected in series at the feed point. This configuration approximates the final configuration envisioned with a bipolar Marx generator. Two ferrite beads on each of the feed cables are used to isolate the feed point from the splitter.

2.2 RF Measurements.

The RF characteristics of the TX-1 were measured on the Farr Research time domain antenna range. The source was a PSPL 4015C, which has a risetime of 20 ps. The source antenna was a TEM-1-50 TEM horn manufactured by Farr Research.. The TX-1 was the receive antenna, and the data was recorded using a Tektronix TDS8000 digital sampling oscilloscope with an 80E04 sampling head. The measurements were made with the antennas 20 meters apart. For comparison, we have included the measurements made earlier on a CIRA-2 [1]. This comparison shows the effects of the large center tube.

In Figure 2.3 we show the TDRs of the two antennas. The TDR at the feed point of the TX-1 shows a large impedance discontinuity, which is due to the close proximity of the two feed cables and the aluminum Marx housing. The ferrite beads had to be placed at least 51 mm (2 in) from the feed point to fit inside the housing. Also, note that the impedance of the feed arms (between the feed point and the resistors) is well below 50 ohms due to the presence of the large conductive center tube.

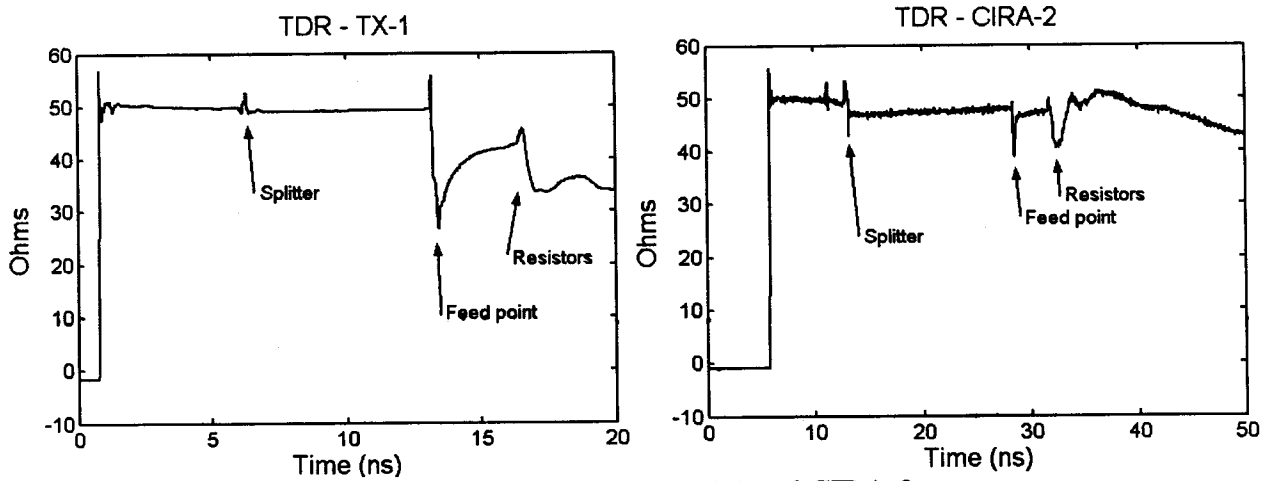

Figure 2.3. TDRs of the TX-1 and CIRA-2.

In Figures 2.4 and 2.5 we show the normalized impulse response in both the time and frequency domains [2]. For the TX-1 we had to set the cutoff frequency for the data processing to 5 GHz, because of high-frequency noise. For the CIRA-2 the cutoff frequency was 12 GHz. The 5 GHz cutoff frequency is still well above the range of interest for this antenna, because of the source risetime. The lower frequency response is probably due to inaccuracies in the sewing of the reflector, resulting in a reflector that is too deep. Due to the much lower frequency response, the pulse width for the TX-1 impulse response is nearly 2.5 times that of the CIRA-2.

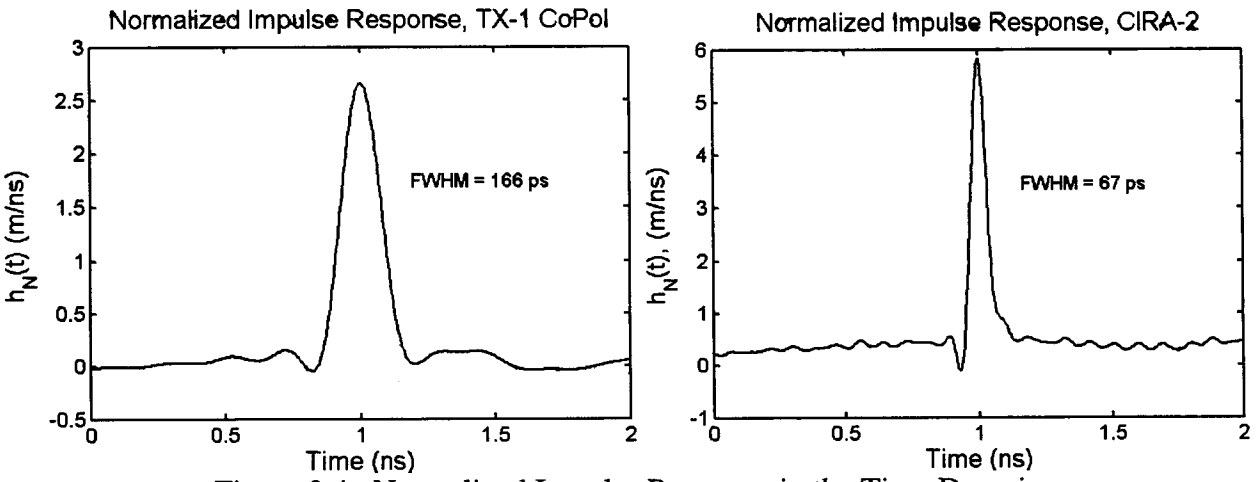

Figure 2.4. Normalized Impulse Response in the Time Domain.

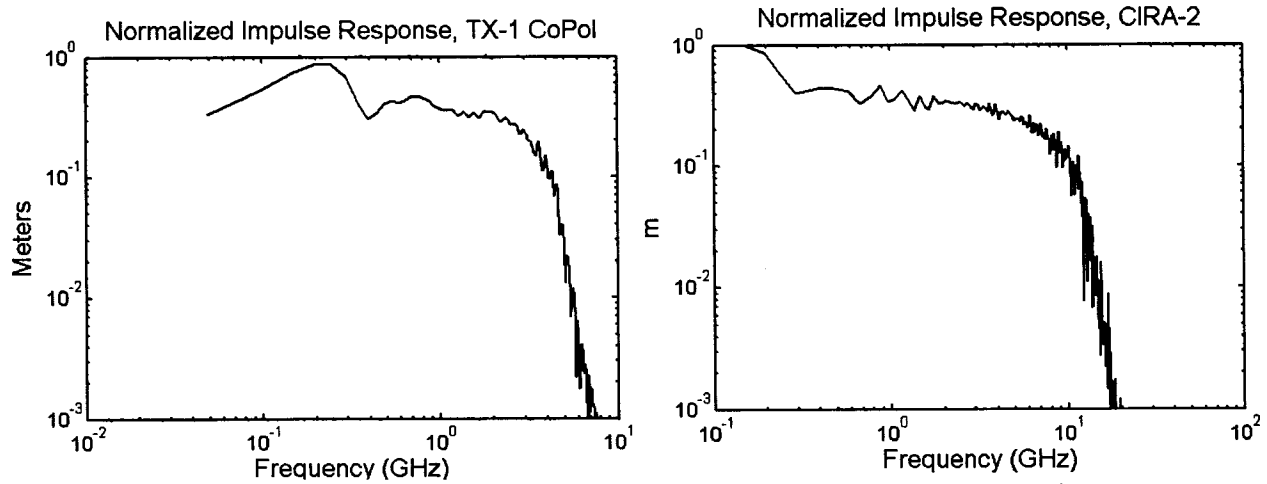

Figure 2.5. Normalized Impulse Response in the Frequency Domain.

Next, we measured the gain of the two reflectors, and the result is shown in Figure 2.6. For the TX-1 we were able to process the data to get the actual gain, but for the CIRA-2 we did not have the reflection coefficient data required to convert to effective gain to gain, so effective gain is shown [2]. The peak gain of the TX-1 is roughly 6 dB below that of the CIRA-2, because of the loss of the high-end response. In addition, the cross-polarization rejection in the TX-1 is much lower than that of the CIRA-2.

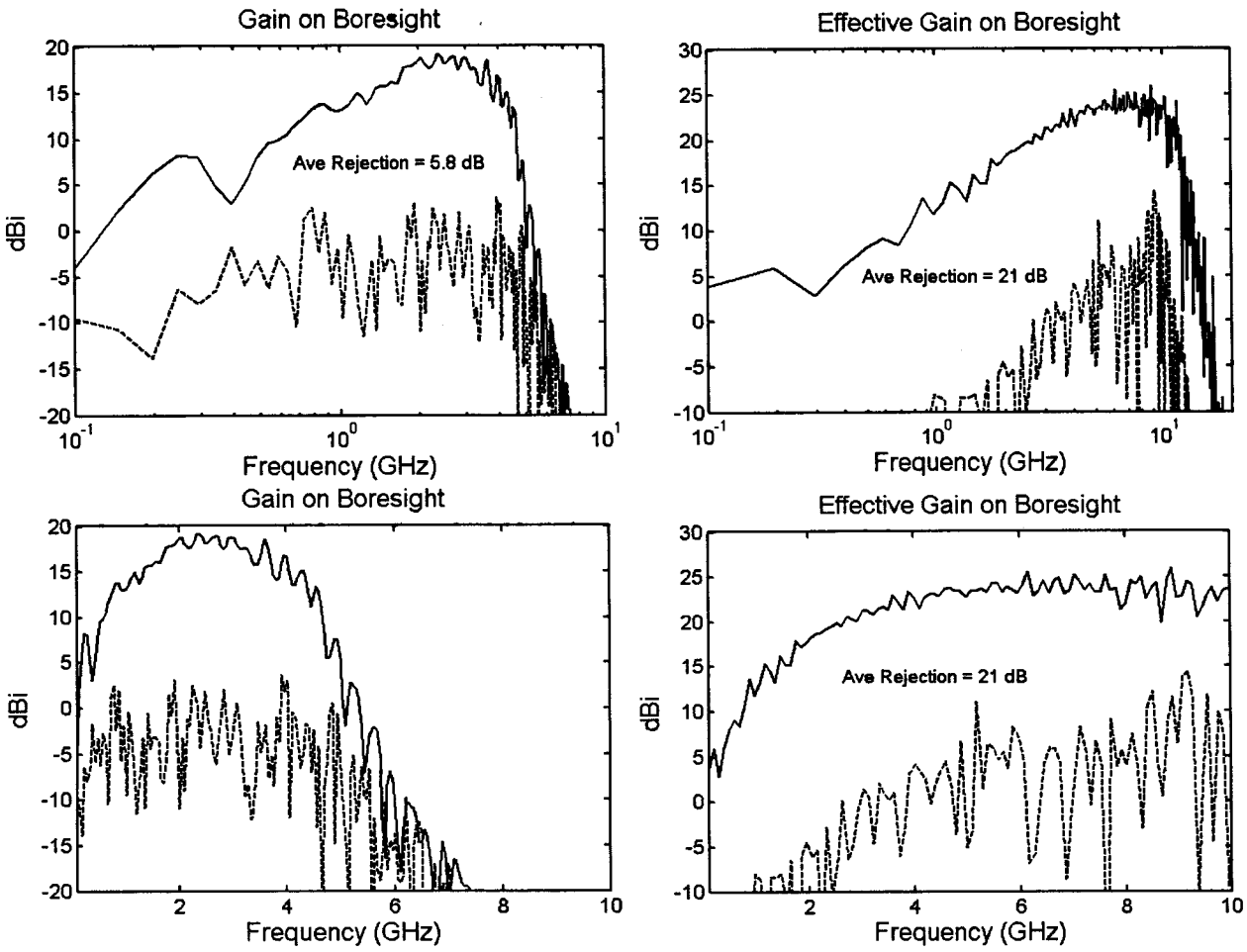

Figure 2.6. Antenna gain and crosspol for the TX-1 (left) and the CIRA-2 antennas, plotted on log (top) and linear (bottom) scales.

Finally, we provide normalized pattern plots for the two antennas, as shown in Figure 2.7. These are not easy to compare, due to the lack of reflection coefficient data on the CIRA-2. The many side lobes in the TX-1 pattern are probably due to the presence of the large center tube and the fact that the reflector is too deep, due to small but consistent and cumulative errors in sewing the reflector panels together.

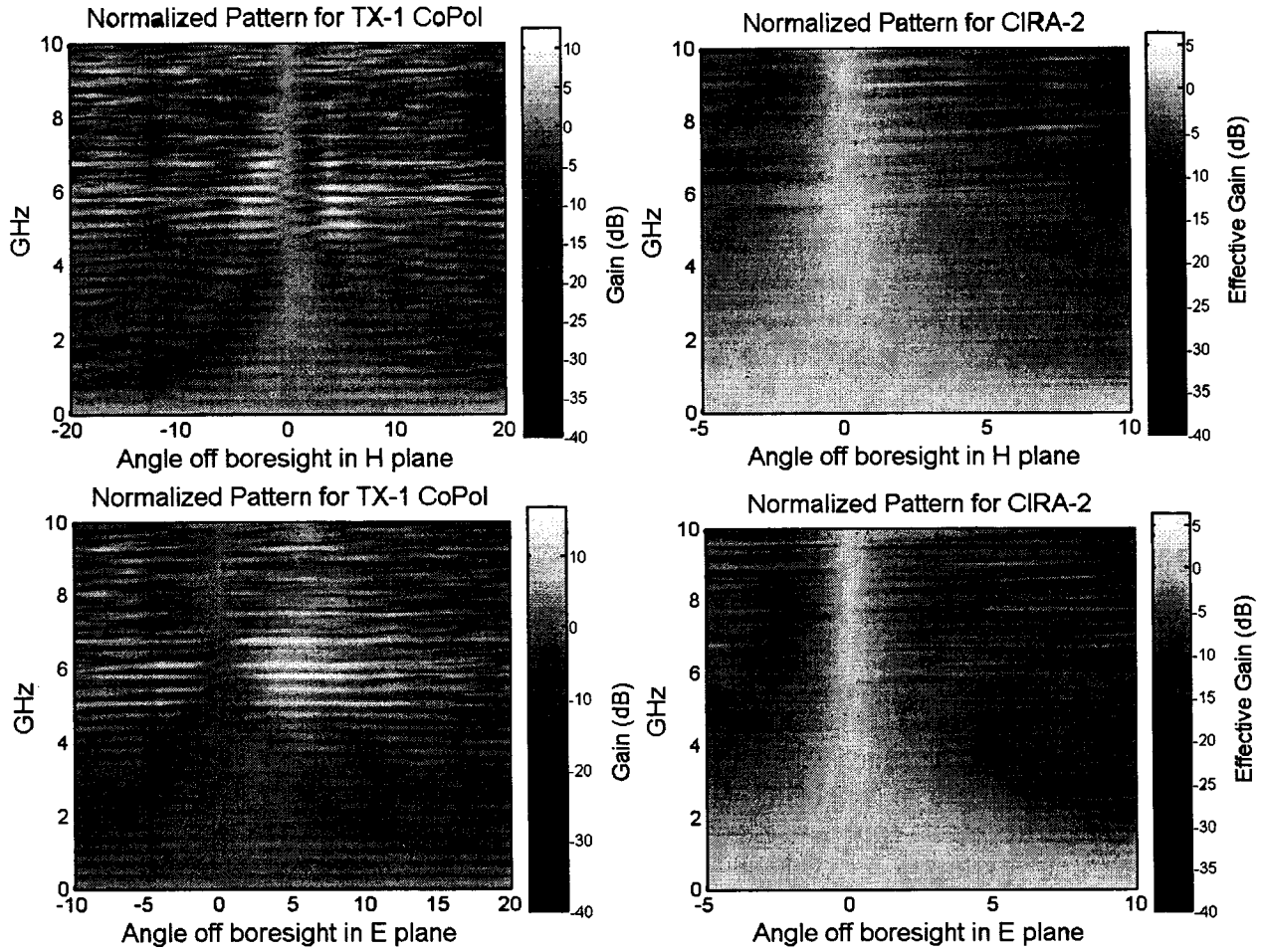

Figure 2.7. Normalized antenna patterns for the TX-1 and CIRA-2.

2.3 Discussion.

Let us determine now whether the 5 GHz bandwidth of the TX-1 is sufficient for the Marx generator. A generator with a risetime of 200 ps has a corresponding frequency spectrum that reaches only as high as 1.75 GHz. The Marx generator reported below has a risetime of approximately 250 ps, so a risetime of 200 ps and bandwidth of 1.75 GHz are somewhat optimistic. Based on this, we see that the TX-1 has sufficient bandwidth to accommodate the Marx generator. We plan to reduce the diameter of the closed antenna in future versions. During Phase II we will fit the center tube to the Marx generator and add a spring mechanism to open the antenna automatically.

3. Bipolar Marx Generator.

The antenna for this project normally requires a positive and negative high-voltage driving pulse. We face the choice of using either a single-polarity or dual-polarity Marx generator. Each choice has advantages and challenges associated with it.

The challenge associated with a single-polarity generator is that we may have to split the output into two new outputs. In this case, we would have to invert one of the new outputs to get both polarities. Another possibility would be to ignore the mismatch at the feed point and use a single polarity feed as described in the Section 4. As will be seen, this may be a reasonable choice.

The challenge associated with a dual-polarity Marx generator lies in timing the two output pulses to occur simultaneously. Based on the anticipated difficulty in splitting and inverting the required high-voltage pulse, we chose initially to investigate a dual polarity Marx.

3.1 Bipolar Marx Description.

Applied Physical Electronics (APE) designed and built the bipolar Marx shown in Figure 3.1. The Marx has positive and negative outputs with about 200 kV peak voltage and risetimes of about 250 ps. Each side of the Marx has ten stages and each side is charged to ±30 kV. The outputs are on opposite ends of the generator, and they run into axial RG-214 cables. The high-voltage supply, triggering, and pressured gas connections are in the center section. The first spark gap for each of the two Marx capacitor banks was shared, in order to reduce jitter between the two sides. The device was filled with dry breathable air.

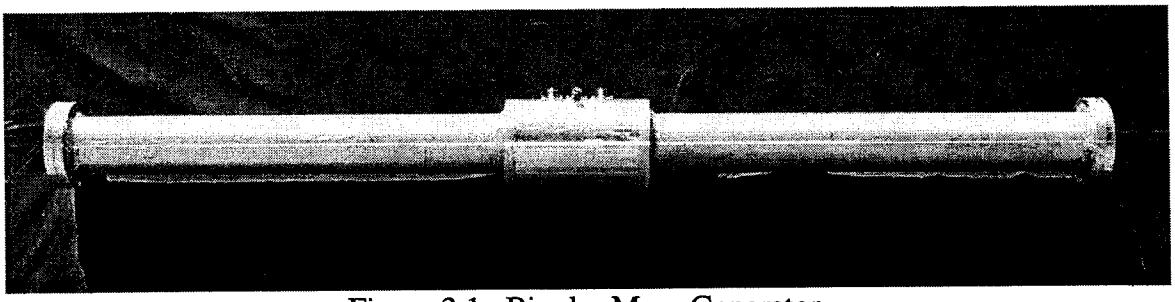

Figure 3.1. Bipolar Marx Generator.

3.2 Bipolar Marx Wave Shape.

APE tested the Marx and provided the data presented here. They measured the Marx outputs by recording the voltage across current viewing resistors (CVRs), which were inserted into a circumferential gap in the output cable braid. A CVR is simply a very low resistance (34 milliohms in this case) inserted in series into a circuit. The low resistance is formed by placing many resistors in parallel. The CVR forms a voltage divider in series with the load resistance, so the voltage across the CVR is directly proportional to the Marx output. APE processed the data to show the output voltage. We plot the complete time record in Figure 3.2 and we expand the leading edge and align the peaks in Figure 3.3. In these plots we invert the negative data to better compare the two outputs.

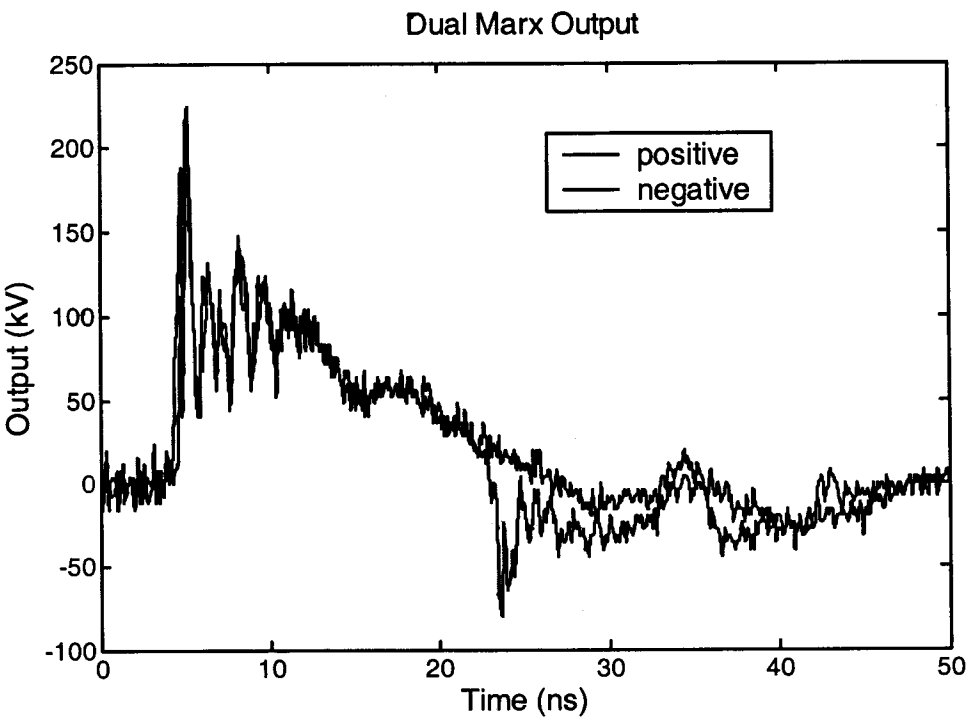

Figure 3.2. Bipolar Marx output.

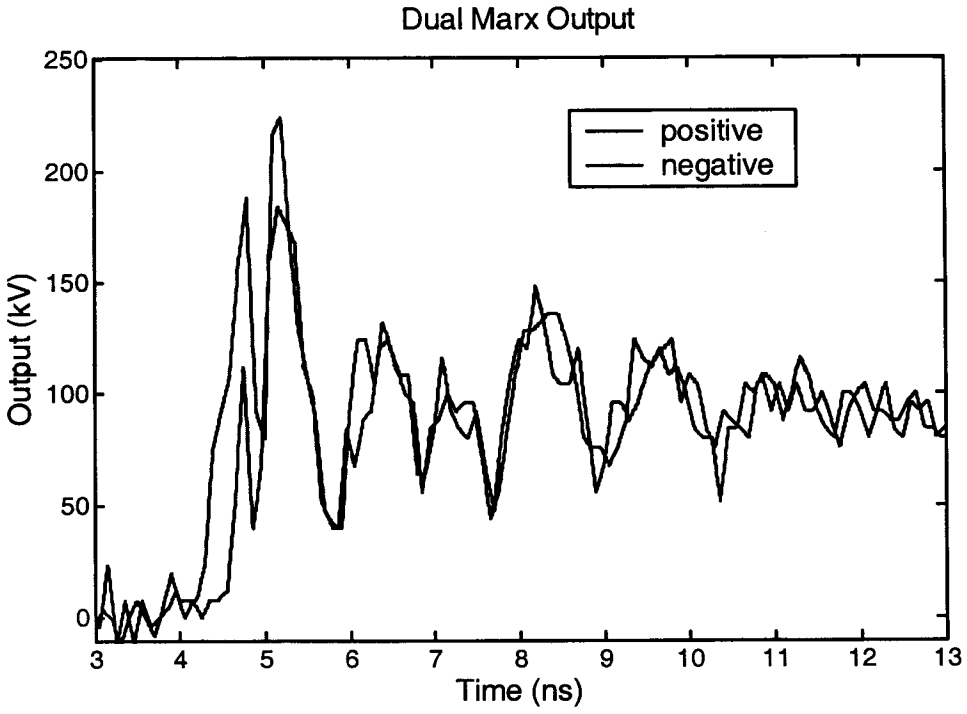

Figure 3.3. Bipolar Marx outputs aligned for maximum.

Alignment of the peaks is necessary to produce the largest generator output potential. The figures show that the generator outputs are not identical, but maximum differential output is the goal — not necessarily just matched outputs.

We further expand the leading edge of the data in Figure 3.4 to measure the risetime. This is difficult to measure for this data, but 250 ps for any given peak is a fair estimate. A 10% to 90% risetime measurement would exceed 500 ps because of the double peak. The 10% point occurs on the rise of the first peak, and the 90% point occurs on the rise of the second peak, resulting in an overly pessimistic number. Note that the data are sampled only every 100 ps, so we may be missing some details that would affect the risetime measurement.

Finally, we plot the total output voltage in Figure 3.5, by aligning and subtracting the two outputs. This perfect alignment produces the 400 kV peak output shown in Figure 3.5. In practice, we will align the two traces by trimming the output cables. There is always some jitter between the positive and negative outputs, so the maximum output will not occur on all pulse pairs.

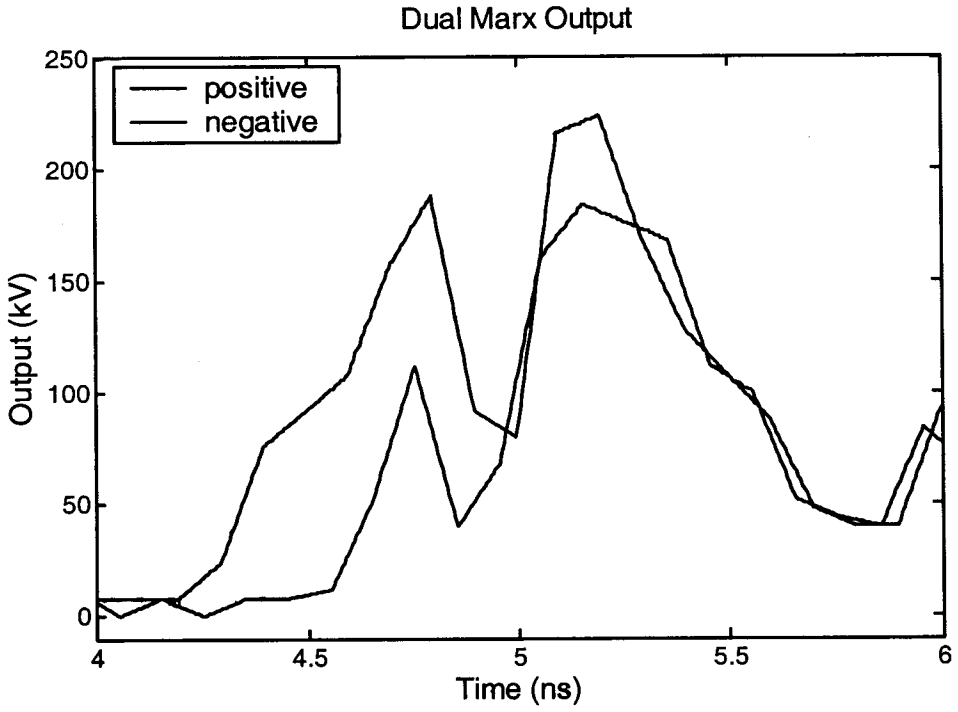

Figure 3.4. Bipolar Marx output expanded to estimate risetime.

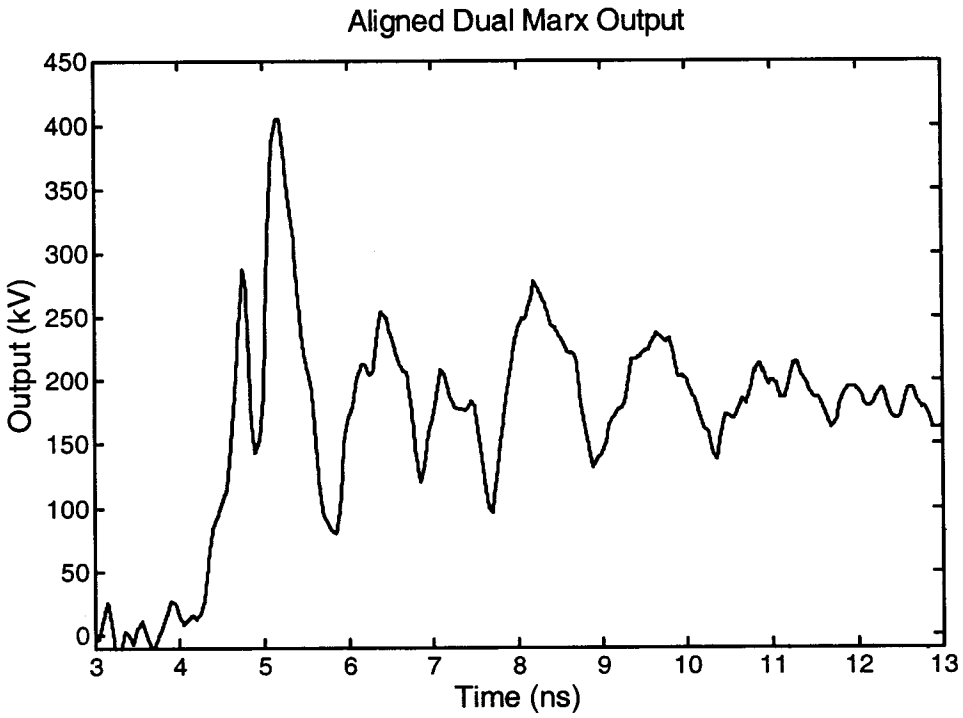

Figure 3.5. Differential output after alignment.

3.3 Bipolar Marx Jitter.

APE measured the jitter between the positive and negative output pulses. The jitter – the difference in time between the positive and negative outputs – is a statistical quantity that can be minimized but not eliminated. The amount of jitter is characterized by the standard deviation of the time difference between the two sides.

APE made the jitter measurements using unmatched cable lengths, so the negative pulse tends to arrive at the scope about 400 ps before the positive pulse. The time difference between the two Marx output pulses is actually unknown, because of the unmatched cable lengths. But this is not a limitation, because the only quantity of interest is the relative jitter, as measured by the standard deviation of the time difference. By adjusting the gap spacing and gas pressure, APE minimized the jitter (standard deviation in the arrival times) between the two pulses. With a minimized standard deviation, we can ultimately trim the cable lengths to time the two pulses to arrive at approximately the same time.

To measure the time difference between the two pulses, APE measured the time halfway up each pulse and recorded the time difference between the positive and negative pulses. They reported jitter measurements for two Marx gas pressures, 210 psi and 225 psi. They measured 40 output pulse pairs at 210 psi, and 10 output pulse pairs at 225 psi, and the results are compiled in Table 4.1

Table 4.1. Bipolar Marx Jitter Measurements

	Pressure	
	210 psi	225 psi
Average time difference (ps)	408	305
Standard Deviation (ps)	122	93

Based the data in Table 4.1, the performance of the bipolar Marx improves with increased pressure. That is, at increased pressure the pulses were more nearly coincident, based on the average time difference. In addition, the jitter is reduced at increased pressure, based on the standard deviation.

From the data, one might suppose that increasing the pressure further would further reduce the jitter, but APE reports that is not the case. They made a few measurements at 250 psi gas pressure. The 250 psi results are not significantly different from the 225 psi results.

We had planned to integrate the bipolar Marx into the TX-1. However, this was not easy to implement because this version of the Marx generator had outputs on opposite ends. It is possible to run long cables from the Marx through the center tube to the feed point of the TX-1, but this is clumsy. A folded version of the bipolar Marx generator would greatly simplify this design. We plan to work on a truly integrated version of the source and antenna in the future.

4. Unbalanced IRA with Single Feed Cable.

We consider now measurements of an IRA with a simplified, unbalanced feed, which may be useful in high-voltage antennas with tight space requirements. IRAs are normally fed by a splitter and two 100-ohm cables connected in parallel at the cable port and in series at the focus. In doing so, one matches a 50-ohm cable to the 200-ohm impedance at the feed point. But such a feed is difficult to build at high voltages or in situations where there is little space, so we consider a simpler feed. Thus, we measure the antenna performance when a 200-ohm IRA-2 is driven by a single 50-ohm cable in an unbalanced configuration.

4.1 Description.

The antenna used for this experiment was a standard Farr Research model IRA-2, shown in Figure 4.1. This antenna has an aluminum reflector with a diameter of 45.7 cm (18 in), and with F/D = 0.5. The feed arms are located at ±30° from the vertical [1]. We built two configurations of IRA-2 with unbalanced feeds. In the first configuration, called IRA-2A1, a single 50-ohm feed cable was run through the center tube that helps support the feed point. We wanted to add a ferrite bead to the feed cable, but there was insufficient room in the center support. In the second configuration, called IRA-2A2, the single feed cable was run down one of

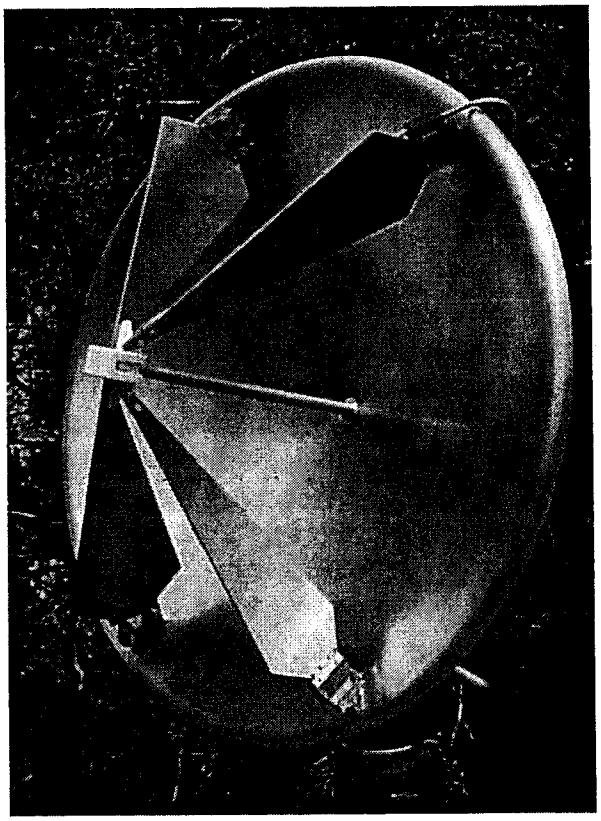

Figure 4.1. A photo of the IRA-2.

the feed arms. This version included a ferrite bead where the cable crossed the load resistors near the edge of the reflector. In both cases, the shield of the feed coax was connected to one pair of feed arms, and the center conductor was connected to the other pair.

4.2 Antenna Measurements.

The RF measurements were made on the Farr Research outdoor time domain antenna range, with the two antennas separated by 10 meters. The equipment used for this test was the same as that described in Section 2.2.

First, we measured the TDRs of the standard IRA-2 and the two versions of the IRA-2 with unbalanced feeds, and the results are shown in Figure 4.2. Next, we measured the impulse response of the three antennas, and the results are shown in Figure 4.3. Of the two unbalanced versions, the one with the cable through the center support tube has the least mismatch and the best impulse response. As one might expect, the TDR and impulse responses with the unbalanced feed are not as good as those with the standard splitter balun. It is interesting to note that the shapes of the impulse responses for the unbalanced versions are very good, although the peaks are somewhat lower than the peak of standard version.

Finally, we measured the effective gain on boresight for the three antennas, and the results are shown in Figure 4.4. We have also included the cross-polarized effective gain for comparison. At frequencies below 12 GHz, there is a only a modest compromise in effective gain with the unbalanced designs. The crosspol gains of the three antennas are somewhat similar to each other. But it is interesting that the crosspol rejection below 7 GHz is better on the unbalanced versions than on the standard version. The crosspol rejection is usually improved by improved symmetry of the antenna, and the IRA-2A1 with the feed cable up the center, has almost perfect symmetry about both of the principal planes [3].

4.3 Discussion.

We have seen that even after accounting for impedance mismatch, the performance (effective gain) of the unbalanced antennas is compromised only modestly at frequencies below 12 GHz. Recall that the best overall measure of an antenna's performance is its effective gain, because it takes into account both antenna gain and impedance mismatch. Since the antennas all work well up to 12 GHz, they cover the frequency range of interest for the Marx source developed here. Recall that these 18-inch diameter antennas are scale models for the 48-inch-diameter TX-1 antenna, so we have to scale the frequencies by 2.67. In section 2.3, we calculate that we require the full-scale TX-1 antenna to have a high-end bandwidth of 1.75 GHz. So the scale model must operate as high as 4.67 GHz, and the scale model actually operates much higher.

There are two situations in which the use of the unbalanced feed may not be appropriate. First, the unbalanced feed designs probably cannot be used in radar applications, because the reflections at the impedance discontinuity tend to generate ghost images. Second, certain sources may be damaged by reflections caused by unbalanced feeds, but that is not the case for the Marx generators studied here.

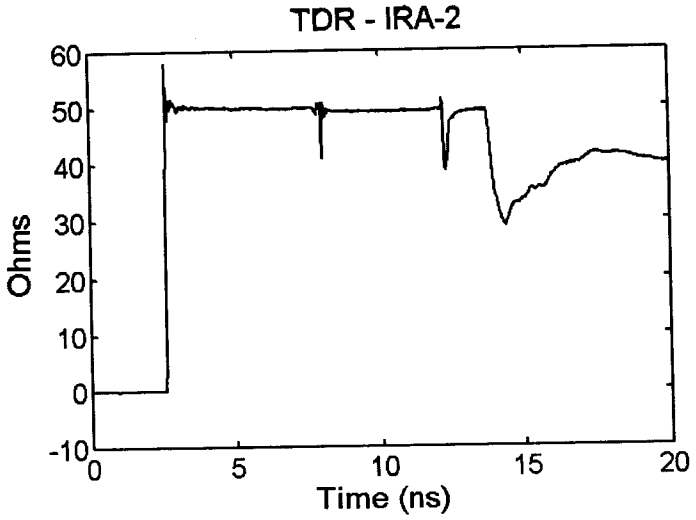
TDR - IRA-2
Ohms
Time (ns)
60
50
40
30
20
10
0
-10
0
5
10
15
20

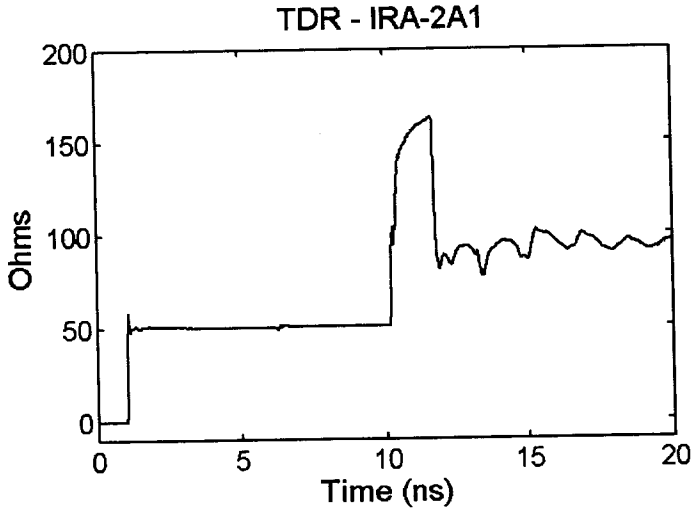
TDR - IRA-2A1
Ohms
Time (ns)
200
150
100
50
0
0
5
10
15
20

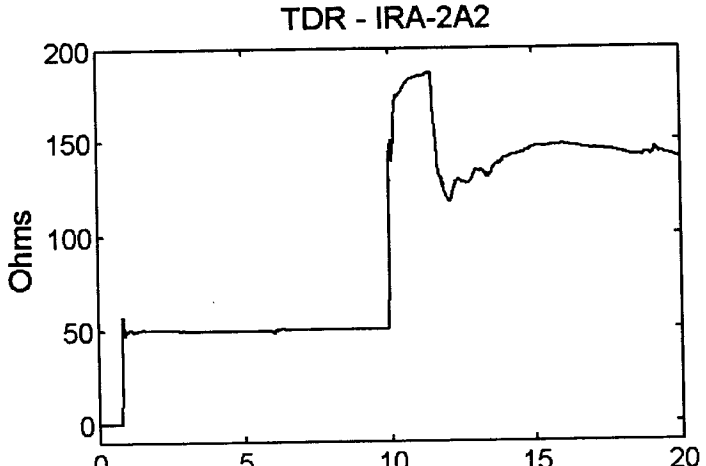
TDR - IRA-2A2
Ohms
200
150
100
50
0
0
5
10
15
20

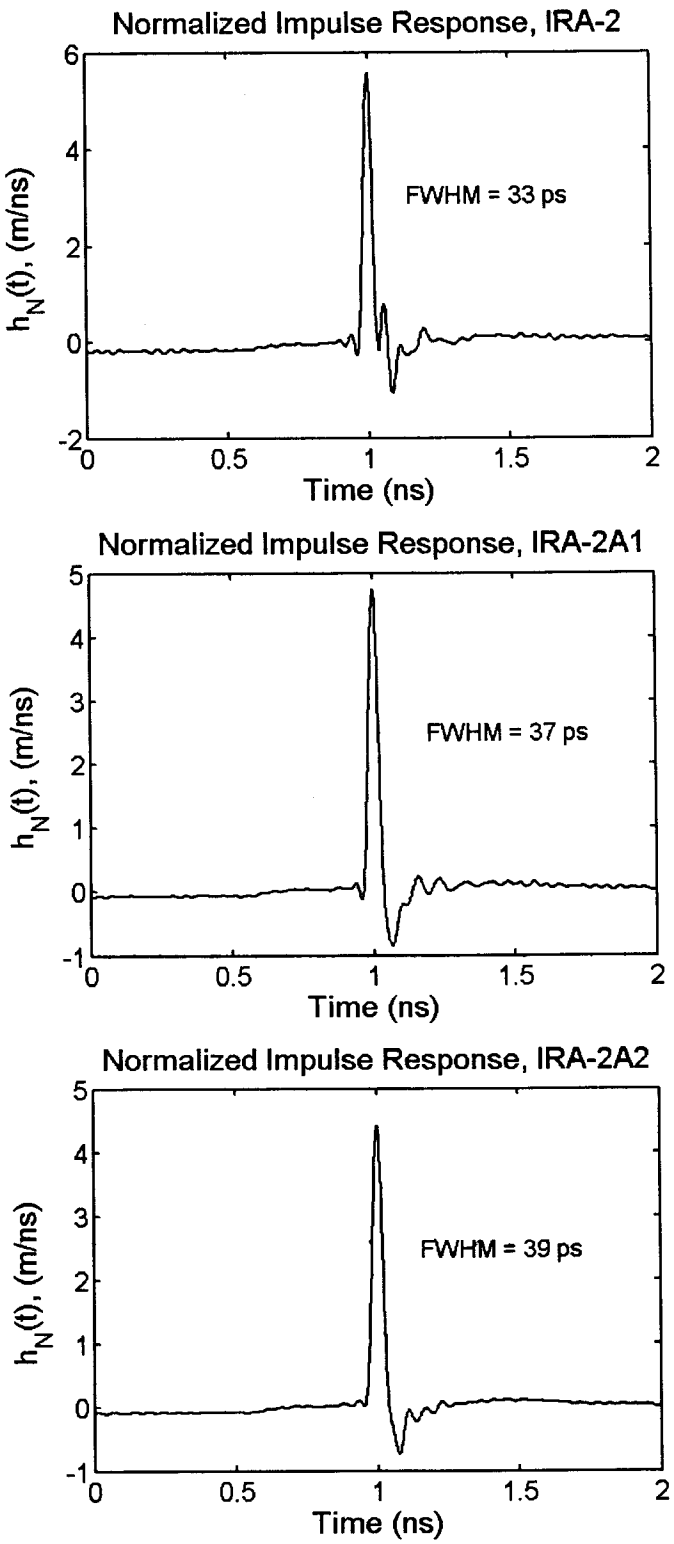

Figure 4.3. Normalized impulse response of IRA-2s with standard feed (top), unbalanced feed through center tube (middle), and unbalanced feed along feed arm (bottom).

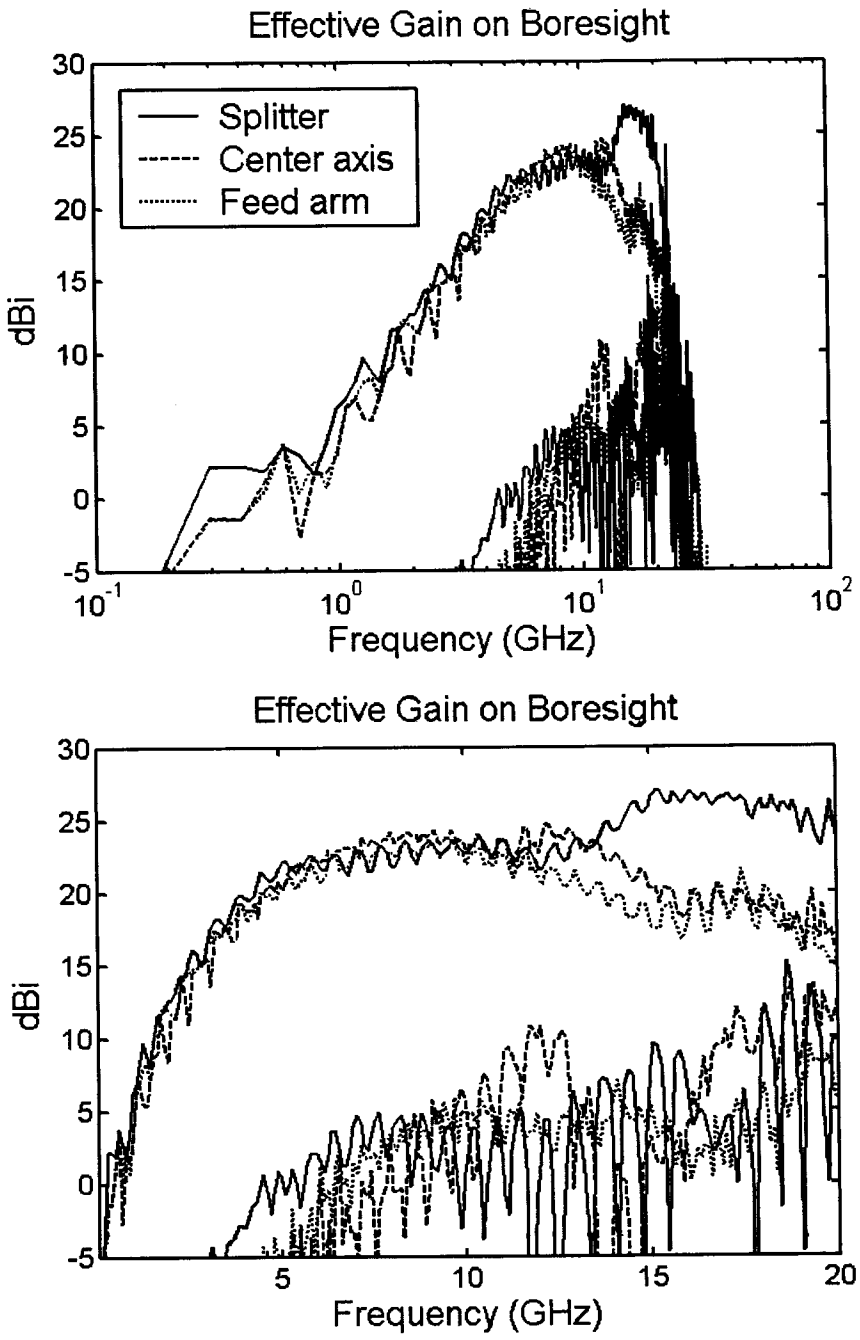

Figure 4.4. Effective gain on boresight including crosspol, for IRA-2s with standard and unbalanced feeds.

5. Conclusions.

We have shown that the TX-1 antenna is a viable antenna for integration with a Marx generator. However, some modifications will be necessary in future versions of the antenna. We plan to reduce the diameter of the center support tube, by fitting the tube to the Marx generator. We also plan to add a spring mechanism to open the antenna automatically. Finally, we plan to use a more sparse mesh in the reflector, to allow even better air flow, which would generate less drag.

The bipolar Marx generator has the required 400 kV bipolar output, provided that the lengths of the output cables are correctly adjusted. To integrate the bipolar Marx into TX-1 antenna, a folded version of the bipolar Marx must be built, so both outputs are located at the same end. Another option is to use a single-output Marx with a sufficient number of stages to maintain the required output voltage. This option is based on the results of Section 4, where we found that a single unbalanced coaxial cable was sufficient to feed an IRA.

In future work, we plan to integrate the Marx into the TX-1 antenna. For this iteration, this was not easy to implement, because the bipolar Marx had the outputs on opposite ends. It would have been possible to run long cables from the Marx through the center tube to the feed point of the TX-1 but this would have been clumsy.

The experiment with unbalanced IRAs has shown that a single coaxial cable is a useful alternative to the splitter balun, causing only a modest compromise in effective gain. It is possible that the reflected signal in unbalanced configurations may damage some sources, however, this is not expected to be a problem for the class of Marx generators considered here.

Acknowledgement

We wish to thank U. S. Army Space and Missile Defense Command for funding this work.

References.

1. L. H. Bowen, E. G. Farr, C. E. Baum, T. C. Tran, and W. D. Prather, Experimental Results of Optimizing the Location of Feed Arms in a Collapsible IRA and a Solid IRA, Sensor and Simulation Note 450, November 2000.
2. L. H. Bowen, E. G. Farr, and W. D. Prather, Fabrication and Testing of Two Collapsible Impulse Radiating Antennas, Sensor and Simulation Note 440, December 1999.
3. C. E. Baum, Symmetry in Single-Polarization Reflector Impulse Radiating Antennas, Sensor and Simulation Note 448, July 2000.